Two Dimensional Chirp Like Model

Debasis Kundu *

Abstract

One dimensional (1-D) and two dimensional (2-D) chirp models have received a considerable amount of attention in the Statistical Signal Processing literature. Recently, Grover [10] proposed a one dimensional chirp-like model that behaves similarly to the classical chirp model but can be implemented more conveniently. It is observed that the signals generated by the two models are virtually indistinguishable. In this paper we propose a 2-D chirp-like model, and it is observed that it behaves very similar to a 2-D chirp model. We propose a least squares method to estimate the unknown parameters and derive the asymptotic properties of the least squares estimators. It is observed that the computation of the least squares estimators involves solving high-dimensional optimization problem, and it can be quite demanding if the number of components is large. In this paper we have proposed to use the sequential least squares estimators which can be implemented quite conveniently. We derive the asymptotic properties of the sequential least squares estimators, and the convergence rates of the sequential least squares estimators are same as those of the least squares estimators. The asymptotic variances of both the least squares estimators and the sequential least squares estimators attain the Cramer-Rao lower bound under the assumptions of Gaussian errors. Extensive simulations have been performed to show the effectiveness of the proposed methods. We have provided two illustrative examples to show how the proposed method can be used in practice.

Keywords: Sinusoidal model; chirp model; chirp-like model; least squares estimators, asymptotic distribution; Cramer-Rao bound; consistent estimators; sequential procedures.

1 Introduction

One-dimensional (1-D) and two-dimensional (2-D) chirp models play important roles in the statistical signal processing literature. The one component 1-D chirp model can be written

*Department of Mathematics and Statistics, Indian Institute of Technology Kanpur, Pin 208016, India, e-mail: kundu@iitk.ac.in. Corresponding author.

mathematically as follows;

$$y(n) = A\cos(\alpha n + \beta n^2) + B\sin(\alpha n + \beta n^2) + e(n); \qquad n = 1, \ldots, N. \tag{1}$$

Here $\{y(n)\}$ is the real valued signal observed at $n = 1, \ldots, N$, A and B are amplitude parameters, α and β are known as the frequency and frequency rate, respectively. The additive noise $e(n)$'s are independent and identically distributed (i.i.d.) normal random variables with mean zero and finite variance σ^2. A more general multicomponent chirp model has the following form;

$$y(n) = \sum_{k=1}^{r}\{A_k\cos(\alpha_k n + \beta_k n^2) + B_k\sin(\alpha_k n + \beta_k n^2)\} + e(n); \qquad n = 1, \ldots, N. \tag{2}$$

Here the parameters $A_k, B_k, \alpha_k, \beta_k$ have the same interpretations as A, B, α, β, respectively of model (1), for all $k = 1, \ldots, r$.

It may be noted that the chirp model (2) can be viewed as an extension of the sinusoidal model;

$$y(n) = \sum_{k=1}^{p}\{A_k\cos(\alpha_k n) + B_k\sin(\alpha_k n)\} + e(n); \qquad n = 1, \ldots, N. \tag{3}$$

The sinusoidal model has played a significant role in the statistical signal processing and time series analysis, see for example the monograph by Quinn and Hannan [33] and Nandi and Kundu [32], for different applications of the sinusoidal model in various fields. In recent times the elementary chirp rate model has received some attention in the signal processing literature due to its wide applications in various fields. The elementary chirp model can be written as follows;

$$y(n) = \sum_{k=1}^{q}\{A_k\cos(\alpha_k n^2) + B_k\sin(\alpha_k n^2)\} + e(n); \qquad n = 1, \ldots, N. \tag{4}$$

Interested readers are referred to Abratkiewicz [2], Mittal et al. [26, 28], Nandi and Kundu [32] and the references cited therein for various applications and estimation procedures. The elementary chirp model (4) also can be seen as an extension of the chirp model (2).

The 1-D chirp model (2) arises in many applications of signal processing, particularly in sonar, radar and communications. For example, chirp signals are used to estimate trajectories of moving objects with respect to fixed receivers. For instance, consider a radar illuminating a target. Then the transmitted signal will be affected by a phase shift induced by the distance and the relative motion between the target and the receiver. Assuming this motion is continuous and differentiable, the phase shift can be adequately modelled as $\phi(t) = c + \alpha t + \beta t^2$, where α and β are related to speed and acceleration or range and speed depending on what the radar is intended for and on the kind of waveforms transmitted, see for example Rihaczek [35] (page 56 - 65). It leads to the chirp signal model (1). An extensive amount of work can be found in the statistical signal processing literature dealing with different aspects one component (1) and multicomponent (2) chirp models, see for example Abatzoglou [1], Djuric and Kay [7], Gini et al. [9], Saha and Kay [36], Nandi and Kundu [30], Kundu and Nandi [21], Lahiri et al. [23, 24, 25], Grover et al. [11], Dhar et al. [6], Nandi et al. [29], the recent monograph by Nandi and Kundu [32] and the references cited therein.

Several authors have noted that there are certain implementation issues of the chirp model to a real data set particularly when the number of components namely p of the model (2) is large. It involves solving a multidimensional optimization problem. Due to this reason Grover [10], see also Grover et al. [14], introduced a novel chirp-like model. Mathematically, the chirp-like model can be defined as follows;

$$y(n) = \sum_{k=1}^{p}\{A_k \cos(\alpha_k n) + B_k \sin(\alpha_k n)\} + \sum_{k=1}^{q}\{C_k \cos(\beta_k n^2) + D_k \sin(\beta_k n^2)\} + e(n);$$
$$n = 1, \ldots, N. \quad (5)$$

It has been observed by Grover [10] and Grover et al. [14] that the chirp-like model behaves exactly like a chirp model, and the model can be used quite conveniently for data analysis purposes. It has been shown by the authors with extensive studies that it is very difficult to discriminate the signals obtained from a chirp model and from a chirp-like model.

Another extension of the 1-D chirp model (2) is two dimensional (2-D) chirp model and it can be described as follows;

$$y(m,n) = \sum_{k=1}^{r} \{A_k \cos(\alpha_k m + \beta_k m^2 + \gamma_k n + \delta_k n^2) + B_k \sin(\alpha_k m + \beta_k m^2 + \gamma_k n + \delta_k n^2) + e(m,n); \quad m = 1, \ldots, M; \; n = 1, \ldots, N. \quad (6)$$

For one dimensional and two dimensional signals (and noise), we use the same notations. It should not create any confusion, it should be clear from the context. Here $y(m, n)$ is the observed signal at (m, n), and $e(m, n)$'s are i.i.d. normal random variables with mean zero and finite variance σ^2, for $m = 1, \ldots, M$ and $n = 1, \ldots, N$. Here also A_k and B_k are the amplitude parameters, (α_k, γ_k) and (β_k, δ_k) are the frequency and frequency rates, respectively. The model (6) has been used quite extensively in many areas of image processing, particularly in modeling gray images, see for example Grover et al. [12], modeling SAR imaging of moving targets, see Barbarossa et al. [3], in the design of low-power low-range modulation systems in underwater Internet of Things, see Jia et al. [18], Vangelista [39], modeling 2-D electronic spectroscopy peak shapes, see Tekavec et al. [38], Binz et al. [5], modeling classical Newton's rings, see for example Guo and Yang [15] and the references cited there in. Similar to the 1-D chirp model, it has been observed that the implementation of the multicomponent 2-D chirp model is a numerically challenging problem, particularly if p is large, see for example Grover et al. [13] or Shukla et al. [37].

The main aim of this paper is to introduce a novel 2-D chirp-like model as a 2-D extension of the 1-D chirp-like model of Grover et al. [14]. It is observed that the proposed 2-D chirp-like model behaves exactly the same as the 2-D chirp model. For all practical purposes, it is not possible to distinguish the signals obtained from a 2-D chirp model and from a 2-D chirp-like model. On the other hand it is shown that the implementation of 2-D chirp-like model is much less challenging computationally compared to a 2-D chirp model. We have proposed to use least squares estimators (LSEs) as they are the most efficient estimators of the unknown parameters. The LSEs are consistent and their asymptotic variances attain the Cramer-Rao lower bound when the errors are Gaussian. The LSEs can be obtained by solving a multidimensional optimization problem. To overcome that we have proposed to use a sequential procedure, which involves solving only 1-D optimization problem at each stage. The corresponding estimators we call them as the sequential least squares estimators (SLSEs). The computation of the SLSEs becomes quite simple. We have shown that the SLSEs are consistent, and they have the same asymptotic variances as the LSEs. Extensive simulations have been done to show how the proposed estimators perform in practice. One illustrative example has been presented to show how the proposed method can be used in practice.

The rest of the paper is organized as follows. In Section 2 we provide the model and the necessary assumptions. Some examples also have been provided. The LSEs and SLSEs are presented in Sections 3 and 4, respectively. In Section 5 the simulation results have been presented to show the performances of the proposed estimators, and two illustrative examples have been presented in Section 6. Finally we conclude the paper in Section 7.

2 Model Formulation and Applications

The subject of the present paper is to introduce mathematically the following 2-D chirp-like model;

$$\begin{aligned} y(m,n) \;=\; & \sum_{j=1}^{p}\{A_j\cos(\alpha_j m+\beta_j n)+B_j\sin(\alpha_j m+\beta_j n)\}+ \\ & \sum_{k=1}^{q}\{C_k\cos(\gamma_k m^2+\delta_k n^2)+D_k\sin(\gamma_k m^2+\delta_k n^2)\}+e(m,n); \\ & m=1,\ldots,M; \qquad n=1,\ldots,N. \end{aligned} \tag{7}$$

Here, $\{(\alpha_j,\beta_j), j=1,\ldots,p\}$ are the frequency parameters and $\{(\gamma_k,\delta_k); k=1,\ldots,q\}$ are the elementary chirp parameters or frequency rates, $\{(A_j,B_j); j=1,\ldots,p\}$ and $\{(C_k,D_k); k=1,\ldots,q\}$ are the amplitude parameters. Here p and q denote the number of frequency components, and the number of elementary chirp components, respectively. The error components

$e(m,n)$'s are assumed to be i.i.d. normal random variables with mean zero and variance σ^2. All frequency, chirp-rate, and amplitude parameters are unknown. The objective is to estimate these parameters based on the observed samples $\{y(m,n); m = 1, \ldots, M;\ n = 1, \ldots, N\}$. A typical image plot of the chirp-like model is provided in Figure 1 with the following parameter values: $p = q = 1$, $\alpha_1 = 1.5$, $\beta_1 = 1.25$, $\gamma_1 = 0.005$ and $\delta_1 = 0.001$. Here the errors are i.i.d $N(0,1)$, i.e. a normal distribution with mean zero and variance 1. Note that for Figures 1, 2, 7 and 8 the x-axis and y-axis denote the values of m and n, respectively. The value of $y(m,n)$ at the point (m,n) is color decoded and the corresponding image plot has been presented.

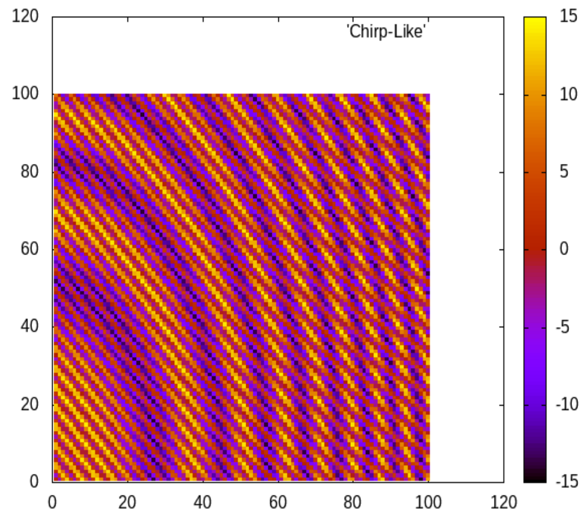

Figure 1: Image plot of two-dimensional chirp-like model (7).

The model (7) is a natural generalization of the 1-D chirp-like model (5) to a chirp-like model in 2-D. Since it is observed that the 1-D chirp-like model behaves very closely with the 1-D chirp model, it is expected that the proposed 2-D chirp-like model (7) with the proper choice of the parameters will behave very closely with the 2-D chirp model (6).

Moreover, the model (7) can be seen as an extension of 2-D sinusoidal model namely

$$
\begin{aligned}
y(m,n) \;&=\; \sum_{j=1}^{p}\{A_j\cos(\alpha_j m+\beta_j n)+B_j\sin(\alpha_j m+\beta_j n)\}+e(m,n);\\
&\qquad\qquad m=1,\ldots,M; \qquad n=1,\ldots,N.
\end{aligned} \tag{8}
$$

It may be mentioned that the 2-D sinusoidal model (8) has received a considerable attention in the signal processing literature during the last two to three decades. It has been used in varied real life applications in the fields of image analysis and restoration, medical imaging, wireless communications, array processing, synthetic aperture radar imaging, texture analysis among others, see for example Hua [17], Barbieri and Barone [4], Francos et al. [8], Rao et al. [34], Kundu and Nandi [20] etc.

Further, note that the model (7) can be seen as an extension of the 2-D elementary chirp model;

$$
\begin{aligned}
y(m,n) \;&=\; \sum_{k=1}^{q}\{C_k\cos(\gamma_k m^2+\delta_k n^2)+D_k\sin(\gamma_k m^2+\delta_k n^2)\}+e(m,n);\\
&\qquad\qquad m=1,\ldots,M; \qquad n=1,\ldots,N.
\end{aligned} \tag{9}
$$

The 2-D elementary chirp model (9) has been used quite extensively in modeling Newton's rings. Newton's ring phenomenon is a classic example of an interference pattern which is created by the reflection of lights between two surfaces, typically a spherical surface and an adjacent touching flat surface. Analyzing this kind of pattern is important in interference fringe analysis. By analyzing Newton's rings one can estimate the curvature radius and position of optical components, refractive index and more. It has been observed that the intensity variation of Newton's rings pattern is of the form

$$
I(m,n) = I_0 + A\cos\left\{\frac{2\pi}{\lambda R}[(m-m_0)^2+(n-n_0)^2]+\pi\right\}, \tag{10}
$$

here I_0 is the mean intensity, A is the amplitude of the cosine variation of the fringes, λ is the incident light wavelength, R is the radius of curvature of the spherical surface, and m_0 and n_0 are the center of Newton's rings, see for example Guo et al. [16], Guo and Yang

[15] and the references cited there in. Clearly, (10) can be obtained as a variant of (9). Extensive amount of work has taken place to analyze the image of Newton's rings and to develop efficient estimation procedures of the unknown parameters from the image of a noisy Newton's rings. A typical Newton's ring with $I_0 = 0.5$, $A = 0.5$, $\lambda = 589.3$, $R = 0.86$ and $m_0 = n_0 = 70$ and with the pixel size 140×140 has been plotted in Figure 2.

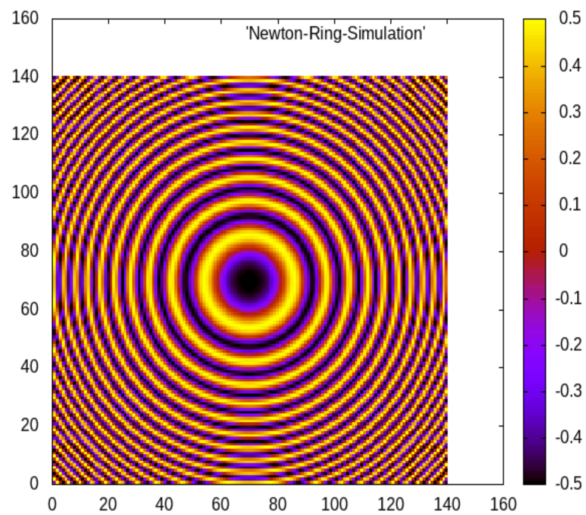

Figure 2: Image plot of the Newton Ring.

3 Least Squares Estimation

In this section we provide the estimation procedure of the unknown parameters of the model (7) based on a random sample $\{y(m,n); m = 1,\ldots,M; n = 1,\ldots,N\}$ and on the error assumption as mentioned before. The model (7) is a typical two dimensional non-linear regression model with an additive error term, hence the least squares method seems to be a natural choice as an estimation method. First we will provide the least squares estimators of the unknown parameters and their asymptotic properties when $p = q = 1$, and then we will provide the results for general p and q.

3.1 Least Squares Estimators: $p = q = 1$

In this case we write the model (7) as follows:

$$\begin{aligned} y(m,n) &= A^0\cos(\alpha^0 m + \beta^0 n) + B^0\sin(\alpha^0 m + \beta^0 n) \\ &\quad + C^0\cos(\gamma^0 m^2 + \delta^0 n^2) + D^0\sin(\gamma^0 m^2 + \delta^0 n^2) + e(m,n). \end{aligned} \tag{11}$$

Here A^0, B^0, C^0 and D^0 are the amplitude parameters, α^0, β^0 are frequencies, and γ^0, δ^0 are elementary chirp parameters as before. Here, A^0, B^0, C^0, D^0, α^0, β^0, γ^0 and δ^0 denote the true value of the parameters. We make this explicit since it is required for deriving the asymptotic distributions of the estimators. The error random variables $e(m,n)$'s are i.i.d. $N(0,\sigma^2)$. We use the following notations: $\boldsymbol{\theta} = (\alpha,\beta)^\top$, $\boldsymbol{\nu} = (A,B)^\top$, $\boldsymbol{\xi} = (\gamma,\delta)^\top$, $\boldsymbol{\eta} = (C,D)^\top$, $\boldsymbol{\theta}^0 = (\alpha^0,\beta^0)^\top$, $\boldsymbol{\nu}^0 = (A^0,B^0)^\top$, $\boldsymbol{\xi}^0 = (\gamma^0,\delta^0)^\top$, $\boldsymbol{\eta}^0 = (C^0,D^0)^\top$. Let

$$\begin{aligned} f(m,n;\boldsymbol{\theta},\boldsymbol{\nu}) &= A\cos(\alpha m + \beta n) + B\sin(\alpha m + \beta n), \\ g(m,n;\boldsymbol{\xi},\boldsymbol{\eta}) &= C\cos(\gamma m^2 + \delta n^2) + D\cos(\gamma m^2 + \delta n^2) \end{aligned}$$

and

$$Q(\boldsymbol{\theta},\boldsymbol{\nu},\boldsymbol{\xi},\boldsymbol{\eta}) = \sum_{m=1}^{M}\sum_{n=1}^{N}\left(y(m,n) - f(m,n;\boldsymbol{\theta},\boldsymbol{\nu}) - g(m,n;\boldsymbol{\xi},\boldsymbol{\eta})\right)^2. \tag{12}$$

Hence, the least squares estimators (LSEs) of the unknown parameters can be obtained by minimizing (12) with respect to the unknown parameters. In this case the LSEs will become the maximum likelihood estimators (MLEs) also as the errors are assumed to be i.i.d. normal distributions. Note that $Q(\boldsymbol{\theta},\boldsymbol{\nu},\boldsymbol{\xi},\boldsymbol{\eta})$ can be written as;

$$Q(\boldsymbol{\theta},\boldsymbol{\nu},\boldsymbol{\xi},\boldsymbol{\eta}) = (\boldsymbol{Y} - \boldsymbol{X}\boldsymbol{\gamma})^\top(\boldsymbol{Y} - \boldsymbol{X}\boldsymbol{\gamma}), \tag{13}$$

here $\boldsymbol{Y}$ and $\boldsymbol{\gamma}$ are vectors of order $MN \times 1$ and 4×1, respectively, and the matrix $\boldsymbol{X}$ is of the order $MN \times 4$ and they are as follows:

$$\boldsymbol{Y}^\top = (y(1,1), y(1,2), \ldots, y(M,1), \ldots, y(M,N)), \boldsymbol{\gamma}^\top = (\boldsymbol{\nu}^\top : \boldsymbol{\eta}^\top), \boldsymbol{X} = [\boldsymbol{X}_1 : \boldsymbol{X}_2 : \boldsymbol{X}_3 : \boldsymbol{X}_4],$$

where $\boldsymbol{X}_1, \boldsymbol{X}_2, \boldsymbol{X}_3, \boldsymbol{X}_4$ are all $MN \times 1$ vectors, and

$$\begin{aligned}
\boldsymbol{X}_1 &= (\cos(\alpha+\beta), \cos(\alpha+2\beta), \ldots, \cos(M\alpha+\beta), \ldots, \cos(M\alpha+N\beta))^\top, \\
\boldsymbol{X}_3 &= (\cos(\gamma+\delta), \cos(\gamma+2^2\delta), \ldots, \cos(M^2\gamma+\delta), \ldots, \cos(M^2\gamma+N^2\delta))^\top.
\end{aligned}$$

Further, $\boldsymbol{X}_2(\boldsymbol{X}_4)$ is same as $\boldsymbol{X}_1(\boldsymbol{X}_3)$ with all the 'cos' terms are replaced by 'sin' terms. Note that the matrices $\boldsymbol{X}_1$ and $\boldsymbol{X}_2$ are functions of $\boldsymbol{\theta}$, and similarly, $\boldsymbol{X}_3$ and $\boldsymbol{X}_4$ are functions of $\boldsymbol{\xi}$. We make it explicit all the times for brevity, whenever it is needed we will make it explicit.

For fixed $\boldsymbol{\theta}$ and $\boldsymbol{\xi}$, the LSE of $\boldsymbol{\gamma}$, say $\widehat{\boldsymbol{\gamma}}(\boldsymbol{\theta}, \boldsymbol{\xi})$ can be obtained as

$$\widehat{\boldsymbol{\gamma}}(\boldsymbol{\theta}, \boldsymbol{\xi}) = \left(\boldsymbol{X}^\top(\boldsymbol{\theta}, \boldsymbol{\xi})\boldsymbol{X}(\boldsymbol{\theta}, \boldsymbol{\xi})\right)^{-1} \boldsymbol{X}^\top(\boldsymbol{\theta}, \boldsymbol{\xi})\boldsymbol{Y}. \tag{14}$$

Hence, the LSEs of $\boldsymbol{\theta}$ and $\boldsymbol{\xi}$ can be obtained by maximizing

$$Q(\boldsymbol{\theta}, \widehat{\boldsymbol{\nu}}(\boldsymbol{\theta}, \boldsymbol{\xi}), \boldsymbol{\xi}, \widehat{\boldsymbol{\eta}}(\boldsymbol{\theta}, \boldsymbol{\xi})) = \boldsymbol{Y}^\top \boldsymbol{X}(\boldsymbol{\theta}, \boldsymbol{\xi}) \left(\boldsymbol{X}^\top(\boldsymbol{\theta}, \boldsymbol{\xi})\boldsymbol{X}(\boldsymbol{\theta}, \boldsymbol{\xi})\right)^{-1} \boldsymbol{X}^\top(\boldsymbol{\theta}, \boldsymbol{\xi})\boldsymbol{Y}. \tag{15}$$

It is a four-dimensional optimization problem. Some simplifications are possible for large M and N, and we are going to explore that. First we would like to study the behavior of the right hand side of (15) for large M and N. Using Lemma 1 and Lemma 3 of Grover et al. [12] it follows that for $0 < \alpha, \beta, \gamma, \delta < \pi$

$$\lim_{\min\{M,N\}\to\infty} \frac{1}{MN} \left(\boldsymbol{X}^\top(\boldsymbol{\theta}, \boldsymbol{\xi})\boldsymbol{X}(\boldsymbol{\theta}, \boldsymbol{\xi})\right) = \frac{1}{2}\boldsymbol{I}. \tag{16}$$

Hence for large M and N, the right hand side of (15) can be approximated as

$$\begin{aligned}
Q_{app}(\boldsymbol{\theta}, \boldsymbol{\xi})) &= \frac{2}{MN}\boldsymbol{Y}^\top \boldsymbol{X}(\boldsymbol{\theta}, \boldsymbol{\xi})\boldsymbol{X}^\top(\boldsymbol{\theta}, \boldsymbol{\xi})\boldsymbol{Y} \\
&= \frac{2}{MN}\boldsymbol{Y}^\top \boldsymbol{X}_1(\boldsymbol{\theta})\boldsymbol{X}_1^\top(\boldsymbol{\theta})\boldsymbol{Y} + \frac{2}{MN}\boldsymbol{Y}^\top \boldsymbol{X}_2(\boldsymbol{\theta})\boldsymbol{X}_2^\top(\boldsymbol{\theta})\boldsymbol{Y} + \\
&\quad \frac{2}{MN}\boldsymbol{Y}^\top \boldsymbol{X}_3(\boldsymbol{\xi})\boldsymbol{X}_3^\top(\boldsymbol{\xi})\boldsymbol{Y} + \frac{2}{MN}\boldsymbol{Y}^\top \boldsymbol{X}_4(\boldsymbol{\xi})\boldsymbol{X}_4^\top(\boldsymbol{\xi})\boldsymbol{Y}.
\end{aligned} \tag{17}$$

Hence, for large M and N, $\widehat{\boldsymbol{\theta}} = (\widehat{\alpha}, \widehat{\beta})$, the LSEs of $\boldsymbol{\theta} = (\alpha, \beta)$, can be obtained by the argument maximum of

$$\begin{aligned} I_1(\alpha,\beta) &= \frac{1}{MN}\boldsymbol{Y}^\top \boldsymbol{X}_1(\boldsymbol{\theta})\boldsymbol{X}_1^\top(\boldsymbol{\theta})\boldsymbol{Y} + \frac{1}{MN}\boldsymbol{Y}^\top \boldsymbol{X}_2(\boldsymbol{\theta})\boldsymbol{X}_2^\top(\boldsymbol{\theta})\boldsymbol{Y}, \\ &= \frac{1}{MN}\left(\sum_{m=1}^{M}\sum_{n=1}^{N} y(m,n)\cos(m\alpha+n\beta)\right)^2 + \frac{1}{MN}\left(\sum_{m=1}^{M}\sum_{n=1}^{N} y(m,n)\sin(m\alpha+n\beta)\right)^2. \end{aligned} \tag{18}$$

Similarly, $\widehat{\boldsymbol{\xi}} = (\widehat{\gamma}, \widehat{\delta})$, the LSE of $\boldsymbol{\xi} = (\gamma, \delta)$, can be obtained as the argument maximum of

$$\begin{aligned} I_2(\gamma,\delta) &= \frac{1}{MN}\left(\boldsymbol{Y}^\top \boldsymbol{X}_3(\boldsymbol{\xi})\boldsymbol{X}_3^\top(\boldsymbol{\xi})\boldsymbol{Y} + \boldsymbol{Y}^\top \boldsymbol{X}_4(\boldsymbol{\xi})\boldsymbol{X}_4^\top(\boldsymbol{\xi})\boldsymbol{Y}\right) \\ &= \frac{1}{MN}\left(\sum_{m=1}^{M}\sum_{n=1}^{N} y(m,n)\cos(m^2\gamma+n^2\delta)\right)^2 + \frac{1}{MN}\left(\sum_{m=1}^{M}\sum_{n=1}^{N} y(m,n)\sin(m^2\gamma+n^2\delta)\right)^2. \end{aligned} \tag{19}$$

Hence, the LSEs of $\boldsymbol{\theta}$ and $\boldsymbol{\xi}$ can be obtained by solving two 2-D optimization problems. Note that for $i = \sqrt{-1}$, $I_1(\alpha, \beta)$ and $I_2(\gamma, \delta)$, can be written as

$$I_1(\alpha,\beta) = \frac{1}{MN}\left|\sum_{m=1}^{M}\sum_{n=1}^{N} y(m,n)e^{i(m\alpha+n\beta)}\right|^2, \tag{20}$$

$$I_2(\gamma,\delta) = \frac{1}{MN}\left|\sum_{m=1}^{M}\sum_{n=1}^{N} y(m,n)e^{i(m^2\gamma+n^2\delta)}\right|^2. \tag{21}$$

Once $\widehat{\boldsymbol{\theta}}$ and $\widehat{\boldsymbol{\xi}}$ are obtained then for large M and N, $\widehat{\boldsymbol{\gamma}}$, the LSE of $\boldsymbol{\gamma}$ can be obtained as

$$\widehat{\boldsymbol{\gamma}}^\top = \frac{2}{MN}\left[\boldsymbol{X}_1(\widehat{\boldsymbol{\theta}})\boldsymbol{Y} : \boldsymbol{X}_2(\widehat{\boldsymbol{\theta}})\boldsymbol{Y} : \boldsymbol{X}_3(\widehat{\boldsymbol{\xi}})\boldsymbol{Y} : \boldsymbol{X}_4(\widehat{\boldsymbol{\xi}})\boldsymbol{Y}\right]. \tag{22}$$

Hence, for large M and N, the LSEs of A, B, C and D become

$$\widehat{A} = \frac{2}{MN}\sum_{m=1}^{M}\sum_{n=1}^{N} y(m,n)\cos(m\widehat{\alpha}+n\widehat{\beta}), \widehat{B} = \frac{2}{MN}\sum_{m=1}^{M}\sum_{n=1}^{N} y(m,n)\sin(m\widehat{\alpha}+n\widehat{\beta}), \tag{23}$$

$$\widehat{C} = \frac{2}{MN}\sum_{m=1}^{M}\sum_{n=1}^{N} y(m,n)\cos(m^2\widehat{\gamma}+n\widehat{\delta}), \widehat{D} = \frac{2}{MN}\sum_{m=1}^{M}\sum_{n=1}^{N} y(m,n)\cos(m\widehat{\gamma}+n\widehat{\delta}). \tag{24}$$

Now we provide the asymptotic properties of the LSEs.

Theorem 1: Suppose there exists a K, such that $K < \infty$, and $0 < |A^0|, |B^0|, |C^0|, |D^0| < K$, and $0 < \alpha^0, \beta^0, \gamma^0, \delta^0 < \pi$. If $e(m, n)$'s are i.i.d. $N(0, \sigma^2)$, then the LSEs are consistent.

Proof: See in the Appendix B. ∎

Theorem 2: Under the same assumptions as in Theorem 1, as $\min\{M,N\} \to \infty$

$$\{M^{1/2}N^{1/2}(\widehat{A}-A^0), M^{1/2}N^{1/2}(\widehat{B}-B^0), M^{3/2}N^{1/2}(\widehat{\alpha}-\alpha^0), M^{1/2}N^{3/2}(\widehat{\beta}-\beta^0)\} \xrightarrow{d} N_4(\mathbf{0}, 2\sigma^2\boldsymbol{\Sigma}_1^{-1}).$$

Here $\xrightarrow{d}$ denotes converges in distribution and $N_4(\mathbf{0}, \boldsymbol{A})$ denotes a 4-variate normal distribution with the mean vector zero, and the dispersion matrix $\boldsymbol{A}$. The matrix $\boldsymbol{\Sigma}_1$ has the following structure;

$$\boldsymbol{\Sigma}_1 = \begin{bmatrix} 1 & 0 & \frac{1}{2}B^0 & \frac{1}{2}B^0 \\ 0 & 1 & -\frac{1}{2}A^0 & -\frac{1}{2}A^0 \\ \frac{1}{2}B^0 & -\frac{1}{2}A^0 & \frac{1}{3}(A^{0^2}+B^{0^2}) & \frac{1}{4}(A^{0^2}+B^{0^2}) \\ \frac{1}{2}B^0 & -\frac{1}{2}A^0 & \frac{1}{4}(A^{0^2}+B^{0^2}) & \frac{1}{3}(A^{0^2}+B^{0^2}) \end{bmatrix}. \tag{25}$$

Also, as $\min\{M,N\} \to \infty$,

$$\{M^{1/2}N^{1/2}(\widehat{C}-C^0), M^{1/2}N^{1/2}(\widehat{D}-D^0), M^{5/2}N^{1/2}(\widehat{\gamma}-\gamma^0), M^{1/2}N^{5/2}(\widehat{\delta}-\delta^0)\} \xrightarrow{d} N_4(\mathbf{0}, 2\sigma^2\boldsymbol{\Sigma}_2^{-1}),$$

where $\boldsymbol{\Sigma}_2$ has the following structure;

$$\boldsymbol{\Sigma}_2 = \begin{bmatrix} 1 & 0 & \frac{1}{3}D^0 & \frac{1}{3}D^0 \\ 0 & 1 & -\frac{1}{3}C^0 & -\frac{1}{3}C^0 \\ \frac{1}{3}D^0 & -\frac{1}{3}C^0 & \frac{1}{6}(C^{0^2}+D^{0^2}) & \frac{1}{9}(C^{0^2}+D^{0^2}) \\ \frac{1}{3}D^0 & -\frac{1}{3}C^0 & \frac{1}{9}(C^{0^2}+D^{0^2}) & \frac{1}{6}(C^{0^2}+D^{0^2}) \end{bmatrix}. \tag{26}$$

Further, the two sets are independently distributed.

Proof: See in the Appendix B. ∎

It may be noted that

$$\boldsymbol{\Sigma}_1^{-1} = \frac{1}{A^{0^2}+B^{0^2}} \begin{bmatrix} A^{0^2}+7B^{0^2} & -6A^0B^0 & -6B^0 & -6B^0 \\ -6A^0B^0 & 7A^{0^2}+B^{0^2} & 6A^0 & 6A^0 \\ -6B^0 & 6A^0 & 12 & 0 \\ -6B^0 & 6A^0 & 0 & 12 \end{bmatrix}. \tag{27}$$

$$\mathbf{\Sigma}_2^{-1} = \frac{1}{C^{0^2} + D^{0^2}} \begin{bmatrix} C^{0^2} + 5D^{0^2} & -4C^0D^0 & -6D^0 & -6D^0 \\ -4C^0D^0 & 5C^{0^2} + D^{0^2} & 6C^0 & 6C^0 \\ -6D^0 & 6C^0 & 18 & 0 \\ -6D^0 & 6C^0 & 0 & 18 \end{bmatrix}. \tag{28}$$

The diagonal entries of $2\sigma^2\mathbf{\Sigma}_1^{-1}$ and $2\sigma^2\mathbf{\Sigma}_2^{-1}$ are the corresponding Cramer-Rao lower bounds. Hence, it implies that the asymptotic variances of the unknown parameters reach the corresponding Cramer-Rao lower bounds.

3.2 Least Squares Estimators for General p and q

In this case we consider LSEs of the general model (7). We use the following notations: $\boldsymbol{\theta}_j = (\alpha_j, \beta_j)^\top$, $\boldsymbol{\nu}_j = (A_j, B_j)^\top$, $\boldsymbol{\theta}_j^0 = (\alpha_j^0, \beta_j^0)^\top$, $\boldsymbol{\nu}_j^0 = (A_j^0, B_j^0)^\top$, for $j = 1, \ldots, p$ and $\boldsymbol{\xi}_k = (\gamma_k, \delta_k)^\top$, $\boldsymbol{\eta}_k = (C_k, D_k)^\top$, $\boldsymbol{\xi}_k^0 = (\gamma_k^0, \delta_k^0)^\top$, $\boldsymbol{\eta}_k^0 = (C_k^0, D_k^0)^\top$ for $k = 1, \ldots, q$. Further, let $\mathbf{\Psi}_1 = (\boldsymbol{\theta}_1, \ldots, \boldsymbol{\theta}_p)$, $\mathbf{\Psi}_2 = (\boldsymbol{\nu}_1, \ldots, \boldsymbol{\nu}_p)$, $\mathbf{\Psi}_3 = (\boldsymbol{\xi}_1, \ldots, \boldsymbol{\xi}_q)$ and $\mathbf{\Psi}_4 = (\boldsymbol{\eta}_1, \ldots, \boldsymbol{\eta}_q)$.

$$\begin{aligned} f(m, n; \boldsymbol{\theta}, \boldsymbol{\nu}) &= A\cos(\alpha m + \beta n) + B\sin(\alpha m + \beta n), \\ g(m, n; \boldsymbol{\xi}, \boldsymbol{\eta}) &= C\cos(\gamma m^2 + \delta n^2) + D\cos(\gamma m^2 + \delta n^2). \end{aligned}$$

The LSEs of the unknown parameters can be obtained by minimizing

$$Q(\mathbf{\Psi}_1, \mathbf{\Psi}_2, \mathbf{\Psi}_3, \mathbf{\Psi}_4) = \sum_{m=1}^{M}\sum_{n=1}^{N}\left(y(m,n) - \sum_{j=1}^{p} f(m, n; \boldsymbol{\theta}_j, \boldsymbol{\nu}_j) - \sum_{k=1}^{q} g(m, n; \boldsymbol{\xi}_k, \boldsymbol{\eta}_k)\right)^2. \tag{29}$$

It is clear from (29) that the LSEs of the unknown parameters in case of the model (7) can be obtained by solving $2(p+q)$ dimensional optimization problem. In the general case also some simplifications are possible for large M and N. Using Lemma 1, it can be shown similarly as the case $p = q = 1$, that for large M and N, and for $j = 1, \ldots, p$, $\widehat{\boldsymbol{\theta}}_j = (\widehat{\alpha}_j, \widehat{\beta}_j)$, the LSEs of $\boldsymbol{\theta}_j^0 = (\alpha_j^0, \beta_j^0)$, can be obtained by the argument maximum of

$$I_{1j}(\alpha_j, \beta_j) = \frac{1}{MN}\left(\sum_{m=1}^{M}\sum_{n=1}^{N} y(m,n)\cos(m\alpha_j + n\beta_j)\right)^2 + \frac{1}{MN}\left(\sum_{m=1}^{M}\sum_{n=1}^{N} y(m,n)\sin(m\alpha_j + n\beta_j)\right)^2.$$

It may be noted that $\{(\widehat{\alpha}_j, \widehat{\beta}_j); j = 1, \ldots, p\}$ are p local maximum of $I_1(\alpha, \beta)$ as defined in (20). Similarly, for large M and N, and for $k = 1, \ldots, q$, $\widehat{\boldsymbol{\xi}}_k = (\widehat{\gamma}_k, \widehat{\delta}_k)$, the LSE of

$\boldsymbol{\xi}_k^0 = (\gamma_k^0, \delta_k^0)$, can be obtained as the argument maximum of

$$I_{2k}(\gamma_k, \delta_k) = \frac{1}{MN}\left(\sum_{m=1}^{M}\sum_{n=1}^{N} y(m,n)\cos(m^2\gamma_k + n^2\delta_k)\right)^2 + \frac{1}{MN}\left(\sum_{m=1}^{M}\sum_{n=1}^{N} y(m,n)\sin(m^2\gamma_k + n^2\delta_k)\right)^2.$$

In this case also $\{(\widehat{\gamma}_k, \widehat{\delta}_k); k = 1, \ldots, q\}$ are q local maximum of $I_2(\gamma, \delta)$ as defined in (21).

Now we provide the asymptotic properties of the LSEs of the unknown parameters..

Theorem 3: Suppose there exists a K, such that $K < \infty$, and $0 < |A_j^0|, |B_j^0|, |C_k^0|, |D_k^0| < K$, and $0 < \alpha_j^0, \beta_j^0, \gamma_k^0, \delta_k^0 < \pi$, for $j = 1, \ldots, p$ and for $k = 1, \ldots, q$. If $e(m,n)$'s are i.i.d. $N(0, \sigma^2)$, then the LSEs are consistent.

Proof: See in the Appendix B. ∎

Theorem 4: Under the same assumptions as in Theorem 1, as $\min\{M, N\} \to \infty$

$$\{M^{1/2}N^{1/2}(\widehat{A}_j - A_j^0), M^{1/2}N^{1/2}(\widehat{B}_j - B_j^0), M^{3/2}N^{1/2}(\widehat{\alpha}_j - \alpha_j^0), M^{1/2}N^{3/2}(\widehat{\beta}_j - \beta_j^0)\} \xrightarrow{d} N_4(\mathbf{0}, 2\sigma^2\boldsymbol{\Sigma}_{1j}^{-1}).$$

Here $\boldsymbol{\Sigma}_{1j}$ has the same form as $\boldsymbol{\Sigma}_1$ of Theorem 1 and A^0 and B^0 are replaced by A_j^0 and B_j^0, respectively for $j = 1, \ldots, p$. Also, for $k = 1, \ldots, q$, as $\min\{M, N\} \to \infty$

$$\{M^{1/2}N^{1/2}(\widehat{C}_k - C_k^0), M^{1/2}N^{1/2}(\widehat{D}_k - D_k^0), M^{5/2}N^{1/2}(\widehat{\gamma}_k - \gamma_k^0), M^{1/2}N^{5/2}(\widehat{\delta}_k - \delta_k^0)\} \xrightarrow{d} N_4(\mathbf{0}, 2\sigma^2\boldsymbol{\Sigma}_{2j}^{-1}),$$

where $\boldsymbol{\Sigma}_{2j}$ has the same form as $\boldsymbol{\Sigma}_2$ of Theorem 1 and C^0 and D^0 are replaced by C_j^0 and D_j^0, respectively. All the sets of random variables are independently distributed.

Proof: See in the Appendix B. ∎

In the general case also the asymptotic variances of the unknown parameters reach the Cramer-Rao lower bound.

4 Sequential Least Squares Estimators

We propose the following sequential least squares estimators (SLSEs) which have the same asymptotic properties as the LSEs. For implementing the sequential procedure, Without loss of generality it is assumed

$$A_1^{0^2} + B_1^{0^2} > A_2^{0^2} + B_2^{0^2} > \ldots > A_p^{0^2} + B_p^{0^2}, \quad \text{and} \tag{30}$$

$$C_1^{0^2} + D_1^{0^2} > C_2^{0^2} + D_2^{0^2} > \ldots > C_q^{0^2} + D_q^{0^2}. \tag{31}$$

The following algorithm can be used to compute the sequential estimators.

Algorithm 1:

Step 0: Assign $j = 1$ and $k = 1$.

Step 1: If $j < p$ and $k < q$ Goto Step 2. If $j < p$ and $k = q$ Goto Step 4a. If $j = p$ and $k < q$ Goto Step 4b. If $j = p$ and $k = q$; STOP.

Step 2: Obtain $(\widehat{\alpha}, \widehat{\beta})$ which maximizes $I_1(\alpha, \beta)$ as defined in (20) and also obtain $(\widehat{\gamma}, \widehat{\delta})$ which maximizes $I_2(\gamma, \delta)$ as defined in (21). Also compute $I_1(\widehat{\alpha}, \widehat{\beta})$ and $I_2(\widehat{\gamma}, \widehat{\delta})$. If $I_1(\widehat{\alpha}, \widehat{\beta}) > I_2(\widehat{\gamma}, \widehat{\delta})$ goto Step 3a, otherwise go to Step 3b.

Step 3a: Obtain $\widehat{A}$ and $\widehat{B}$ using (23). Replace $y(m, n)$ by

$$y(m, n) - \widehat{A}\cos(\widehat{\alpha}m + \widehat{\beta}n) - \widehat{B}\sin(\widehat{\alpha}m + \widehat{\beta}n).$$

Assign $\widehat{A}_j = \widehat{A}$, $\widehat{B}_j = \widehat{B}$, $\widehat{\alpha}_j = \widehat{\alpha}$, $\widehat{\beta}_j = \widehat{\beta}$. Replace j by $j + 1$ and go to Step 1.

Step 3b: Obtain $\widehat{C}$ and $\widehat{D}$ using (24). Replace $y(m, n)$ by

$$y(m, n) - \widehat{C}\cos(\widehat{\gamma}m^2 + \widehat{\delta}n^2) - \widehat{D}\sin(\widehat{\gamma}m^2 + \widehat{\delta}n^2).$$

Assign $\widehat{C}_k = \widehat{C}$, $\widehat{D}_k = \widehat{D}$, $\widehat{\gamma}_k = \widehat{\gamma}$, $\widehat{\delta}_k = \widehat{\delta}$. Replace k by $k + 1$ and go to Step 1.

Step 4a: Obtain $(\widehat{\alpha}, \widehat{\beta})$ which maximizes $I_1(\alpha, \beta)$ as defined in (20) and repeat Step 3a.

Step 4b: Obtain $(\widehat{\gamma}, \widehat{\delta})$ which maximizes $I_2(\gamma, \delta)$ as defined in (21) and repeat Step 3b.

It is clear that to implement the sequential procedure one needs to solve a 2-D optimization problem at each step. This significantly reduces the computational burden. Even if for large p and q, the proposed sequential procedure can be used in practice quite conveniently. Moreover, it is not difficult to show that the asymptotic properties of the sequential estimators are same as the least squares estimators, i.e. for the sequential estimators also, Theorem 3 and Theorem 4 hold true.

For implementing Algorithm 1, one needs to maximize $I_1(\alpha, \beta)$ and $I_2(\gamma, \delta)$. Here, $0 < \alpha, \beta, \gamma, \delta < \pi$. Both $I_1(\alpha, \beta)$ and $I_2(\gamma, \delta)$ have several local maxima. Hence, it is important to choose the initial guesses so that the iterative process converges to the global optimum rather than the local optimum. In case of $I_1(\alpha, \beta)$ consider the points of the form $\left(\frac{\pi s}{M}, \frac{\pi t}{N}\right)$, for $s = 1, \ldots, M$ and $t = 1, \ldots, N$. Compute $I_1(s, t)$, for all these MN points and choose that point (s_0, t_0) as the initial guess for which $I_1(s_0, t_0)$ is the maximum. Similarly, in case of $I_2(\gamma, \delta)$, consider the points of the form $\left(\frac{\pi s}{M^2}, \frac{\pi t}{N^2}\right)$, for $s = 1, \ldots, M^2$ and $t = 1, \ldots, N^2$. Compute $I_2(s, t)$, for all these M^2N^2 points and choose that point (s_0, t_0) as the initial guess for which $I_2(s_0, t_0)$ is the maximum. Any 2-D optimization algorithm can be used to maximize these two functions.

5 Simulation Results

In this section we present some simulation results to show how the proposed method performs in practice. We have considered the following two models

Model 1:

$$y(m, n) = 1.0 \cos(0.05m^2 + 0.05n^2) + 1.0 \sin(0.05m^2 + 0.05n^2) + e(m, n)$$

and

Model 2:

$$
\begin{aligned}
y(m,n) &= 0.75\cos(1.25m + 1.25n) + 0.75\sin(1.25m + 1.25n) \\
&\quad +1.0\cos(0.05m^2 + 0.05n^2) + 1.0\sin(0.05m^2 + 0.05n^2) + e(m,n).
\end{aligned}
$$

Here $e(m,n)$'s are i.i.d. normal random variables with mean zero and variance σ^2. In both the cases we have considered different sample sizes and different error variances. In each case we have generated the sample and estimate the unknown parameters based on the proposed sequential procedures. We replicate the process 1000 times and report the average estimates and the associated square root of the mean squared errors (SMSE) below the average estimates in brackets. The results for Model 1 are presented in Table 1 and Figure 3, and for Model 2 in Tables 2, 3. and in Figures 4 and 5. In the tables we have presented the average least squares estimates of the different parameters and the corresponding SMSEs have been presented in the figures.

Several observations can be made from the simulation results. In both the cases as the sample size increases or the error variance decreases, the average biases and SMSE decrease. It verifies the consistency properties of all the estimators. Comparing Tables 1 and 3 and Figures 3 and 5, it is observed that the average estimates and SMSE are very close to each other as it is expected. It verifies the asymptotic independence of the two sets of estimates.

Now we would like to compare the time required to compute the LSEs and the SLSEs for the same model. We have provided the ratio of the time required to compute the LSEs and SLSEs for different sample sizes and for different error variances for Model 2, in Figure 6. It is observed that as the sample size and the error variance increase the computational gain to use SLSE becomes more. Hence, it is recommended to use the sequential least squares estimators for all practical purposes.

σ^2	n	C	D	γ	δ
1.00	25	0.9976	1.0034	5.0001E-02	5.0005E-02
	50	0.9993	1.0019	5.0002E-02	5.0001E-02
	75	1.0007	0.9995	5.0000E-02	5.0000E-02
	100	1.0002	1.0001	5.0000E-02	5.0000E-02
1.50	25	0.9969	1.0040	5.0002E-02	5.0006E-02
	50	0.9991	1.0024	5.0002E-02	5.0001E-02
	75	1.0009	0.9994	5.0000E-02	4.9999E-02
	100	1.0002	1.0002	5.0000E-02	5.0000E-02
2.00	25	0.9963	1.0046	5.0002E-02	5.0007E-02
	50	0.9989	1.0027	5.0002E-02	5.0001E-02
	75	1.0010	0.9993	5.0001E-02	4.9999E-02
	100	1.0003	1.0002	5.0000E-02	5.0000E-02
2.50	25	0.9957	1.00450	5.0003E-02	5.0009E-02
	50	0.9988	1.0030	5.0003E-02	5.0001E-02
	75	1.0011	0.9992	5.0001E-02	4.9999E-02
	100	1.0003	1.0003	5.0000E-02	5.0000E-02

Table 1: The Average estimates of $C^0 = 1.0$, $D^0 = 1.0$, $\gamma^0 = 0.05$ and $\delta^0 = 0.05$ for different sample sizes and for different error variances for Model 1.

6 Illustrative Example

6.1 Example 1:

In this section we provide an illustrative example to show how the proposed method can be used in practice. We have simulated a data set from the model (7) with the following model parameters:

$$
\begin{aligned}
p = q = 2, \qquad & M = N = 50, \sigma^2 = 1 \\
& A_1^0 = B_1^0 = 6.0, \alpha_1^0 = \beta_1^0 = 1.25, C_1^0 = D_1^0 = 5.0, \gamma_1^0 = \delta_1^0 = 0.15 \\
& A_2^0 = B_2^0 = 4.0, \alpha_2^0 = \beta_2^0 = 0.75, C_2^0 = D_2^0 = 2.0, \gamma_2^0 = \delta_2^0 = 0.005. \qquad (32)
\end{aligned}
$$

The image plot of the noisy signal has been plotted in Figure 7. The problem is to extract the original signal from the noisy image. We have used the sequential procedure to estimate the unknown parameters. Using the sequential procedure as it has been described

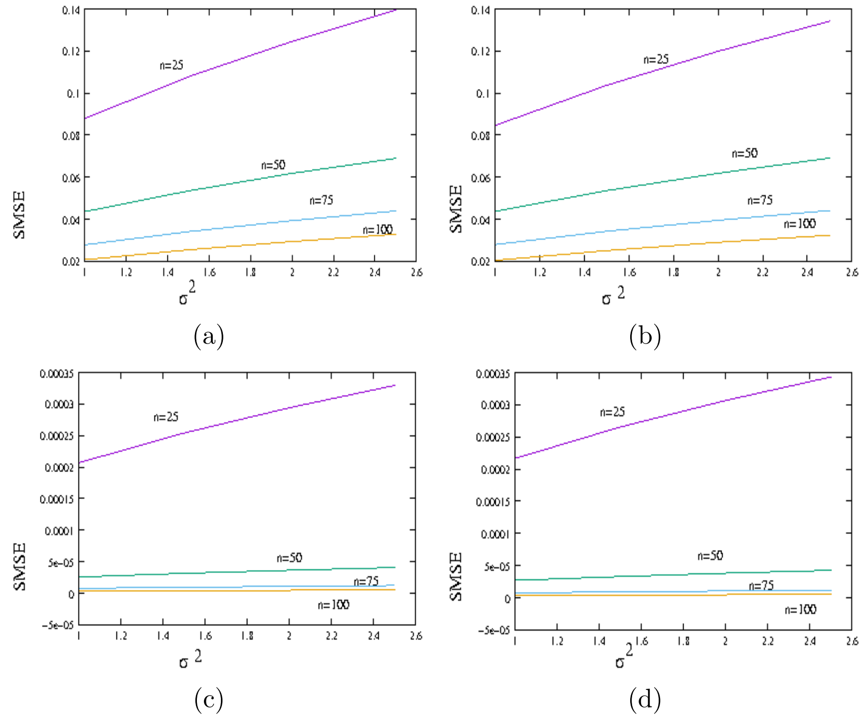

Figure 3: The square root of the mean squared errors of the LSEs of (a) C^0, (b) D^0, (c) γ^0 and (d) δ^0 for different sample sizes and for different error variances for Model 1.

before, first we have obtained $(\widehat{\alpha}_1, \widehat{\beta}_1, \widehat{A}_1, \widehat{B}_1)$, then $(\widehat{\gamma}_1, \widehat{\delta}_1, \widehat{C}_1, \widehat{D}_1)$, then $(\widehat{\alpha}_2, \widehat{\beta}_2, \widehat{A}_2, \widehat{B}_2)$, and finally $(\widehat{\gamma}_2, \widehat{\delta}_2, \widehat{C}_2, \widehat{D}_2)$. The estimates of the unknown parameters and the corresponding 95% confidence intervals have been provided below:

A_1	B_1	α_1	β_1	A_2	B_2	α_2	β_2
6.01354 $\mp$0.57702	5.87012 $\mp$0.58757	1.24995 $\mp$0.01697	1.24957 $\mp$0.01697	3.69511 $\mp$0.62358	4.50515 $\mp$0.53790	0.75193 $\mp$0.02448	0.75131 $\mp$0.02448

C_1	D_1	γ_1	δ_1	C_2	D_2	γ_2	δ_2
5.56339 $\mp$0.58768	5.04637 $\mp$0.52039	0.14998 $\mp$0.00007	0.14998 $\mp$0.00007	1.79644 $\mp$0.53582	2.18495 $\mp$0.47069	0.00508 $\mp$0.00017	0.00501 $\mp$0.00017

We have presented the estimated image based on the above estimated parameter values in Figure 7. They match quite well.

σ^2	n	A	B	α	β
	25	0.6467	0.8411	1.2496	1.2491
1.00	50	0.6140	0.8689	1.2528	1.2528
	75	0.6964	0.8119	1.2508	1.2508
	100	0.7192	0.7978	1.2503	1.2503
	25	0.6447	0.8375	1.2497	1.2491
1.50	50	0.6132	0.8683	1.2528	1.2528
	75	0.6964	0.8114	1.2508	1.2507
	100	0.7193	0.7974	1.2503	1.2503
	25	0.6426	0.8337	1.2497	1.2490
2.00	50	0.6122	0.8679	1.2528	1.2528
	75	0.6963	0.8111	1.2508	1.2507
	100	0.7191	0.7972	1.2503	1.2503
	25	0.6404	0.8302	1.2497	1.2490
2.50	50	0.6113	0.8674	1.2528	1.2528
	75	0.6965	0.8105	1.2508	1.2507
	100	0.7190	0.7970	1.2503	1.2503

Table 2: The average estimates of the LSEs of $A^0 = 0.75$, $B^0 = 0.75$, $\alpha^0 = 1.25$ and $\beta^0 = 1.25$ for different sample sizes and for different error variances for Model 2.

6.2 Example 2:

It has been observed that the famous Newton ring can be modeled by the proposed two dimensional chirp-like model. In this section we consider the noisy Newton ring which is plotted in Figure 8 (a). The main aim is to extract the original Newton ring as in Figure 2 from the noisy Newton ring as in Figure 8 (a). We have used the least squares technique as it has been proposed in this manuscript to estimate the unknown parameters. Based on the least squares estimators the estimated Newton ring is plotted in Figure 8 (b). The estimated Newton ring resembles the original Newton ring quite well.

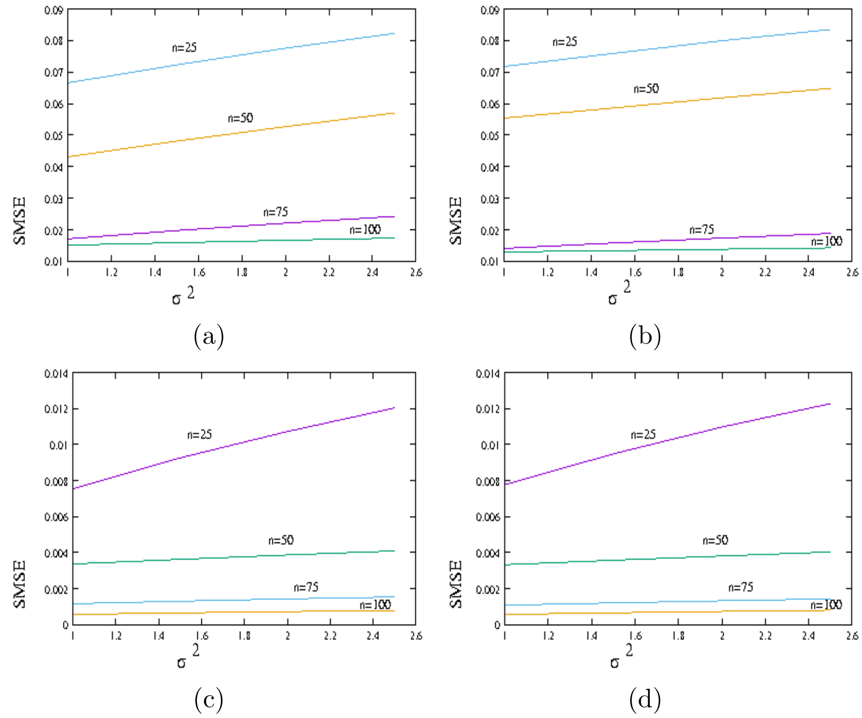

Figure 4: The square root of the mean squared errors of the LSEs of (a) A^0, (b) B^0, (c) γ^0 and (d) δ^0 for different sample sizes and for different error variances for Model 2.

7 Conclusions

In this paper we have proposed a 2-D chirp-like model, and it can be used quite effectively as an alternative to the 2-D chirp model. The results demonstrate that the proposed model can be used in practice more conveniently than the popular 2-D chirp-like model. The 2-D sinusoidal model and the 2-D elementary chirp model can be obtained as special cases of the proposed model. We have proposed a sequential procedure to compute the SLSEs and have established their asymptotic properties. The asymptotic variances of the SLSEs attain the Cramer-Rao lower bound. We have provided two illustrative examples to show how the proposed model can be used in practice. It has been shown that the proposed model can be used quite effectively to model the famous Newton ring.

σ^2	n	C	D	γ	δ
1.00	25	1.0985	0.8691	4.9948E-02	4.9951E-02
	50	1.0412	0.9562	4.9990E-02	4.9989E-02
	75	1.0272	0.9781	5.0000E-02	4.9999E-02
	100	1.0378	0.9731	4.9998E-02	4.9998E-02
1.50	25	1.0978	0.8698	4.9948E-02	4.9953E-02
	50	1.0411	0.9566	4.9991E-02	4.9990E-02
	75	1.0273	0.9780	5.0000E-02	4.9999E-02
	100	1.0379	0.9731	4.9998E-02	4.9998E-02
2.00	25	0.9963	1.0046	5.0002E-02	5.0007E-02
	50	0.9989	1.0027	5.0002E-02	5.0001E-02
	75	1.0010	0.9993	5.0001E-02	4.9999E-02
	100	1.0003	1.0002	5.0000E-02	5.0000E-02
2.50	25	1.0972	0.8702	4.9948E-02	4.9954E-02
	50	1.0409	0.9570	4.9991E-02	4.9990E-02
	75	1.0276	0.9778	5.0001E-02	4.9999E-02
	100	1.0380	0.9731	4.9998E-02	4.9998E-02

Table 3: The average estimates of the LSEs of $C^0 = 1.0$, $D^0 = 1.0$, $\gamma^0 = 0.05$ and $\delta^0 = 0.05$ for different sample sizes and for different error variances for Model 2.

Acknowledgements:

The author would like to thank two unknown reviewers for their constructive comments which have helped to improve the earlier draft of the manuscript significantly.

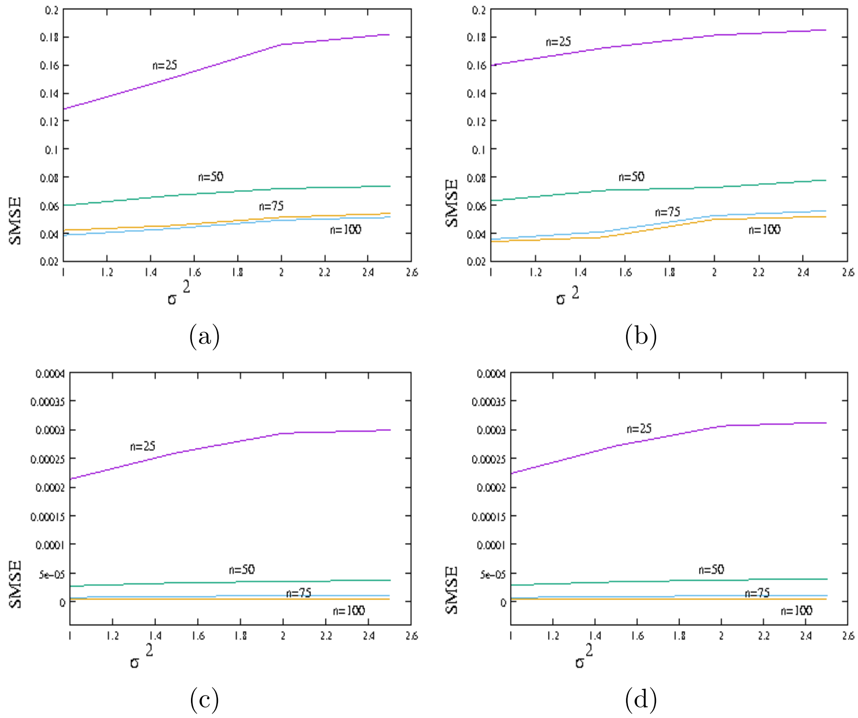

Figure 5: The square root of the mean squared errors of the LSEs of (a) C^0, (b) D^0, (c) γ^0 and (d) δ^0 for different sample sizes and for different error variances for Model 2.

Appendix A: Preliminaries

Lemma 1: If $(\omega_1, \omega_2, \psi_1, \psi_2) \in (0, \pi) \times (0, \pi) \times (0, \pi) \times (0, \pi)$, then except of finite number of points and for $s, t = 0, 1, \ldots$, the following are true:

$$(a) \quad \lim_{\min\{M,N\}\to\infty} \frac{1}{MN} \sum_{m=1}^{M} \sum_{n=1}^{N} \cos(\omega_1 m + \omega_2 n) = \lim_{\min\{M,N\}\to\infty} \frac{1}{MN} \sum_{m=1}^{M} \sum_{n=1}^{N} \sin(\omega_1 m + \omega_2 n) = 0$$

$$(b) \quad \lim_{\min\{M,N\}\to\infty} \frac{1}{MN} \sum_{m=1}^{M} \sum_{n=1}^{N} \cos(\psi_1 m^2 + \psi_2 n^2) = \lim_{\min\{M,N\}\to\infty} \frac{1}{MN} \sum_{m=1}^{M} \sum_{n=1}^{N} \sin(\psi_1 m^2 + \psi_2 n^2) = 0$$

$$(c) \quad \lim_{\min\{M,N\}\to\infty} \frac{1}{MN} \sum_{m=1}^{M} \sum_{n=1}^{N} \cos^2(\omega_1 m + \omega_2 n) = \lim_{\min\{M,N\}\to\infty} \frac{1}{MN} \sum_{m=1}^{M} \sum_{n=1}^{N} \sin^2(\omega_1 m + \omega_2 n) = \frac{1}{2}$$

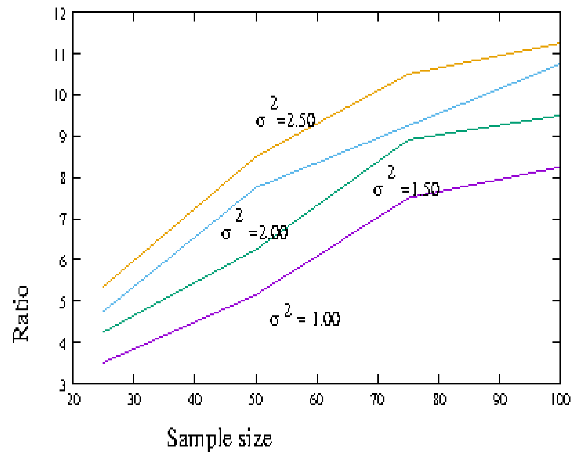

Figure 6: Ratio of the time required to compute the LSEs and SLSEs for different sample sizes and for different error variances for Model 2.

$$(d)\quad \lim_{\min\{M,N\}\to\infty} \frac{1}{MN}\sum_{m=1}^{M}\sum_{n=1}^{N}\cos^2(\psi_1 m^2+\psi_2 n^2) = \lim_{\min\{M,N\}\to\infty} \frac{1}{MN}\sum_{m=1}^{M}\sum_{n=1}^{N}\sin^2(\psi_1 m^2+\psi_2 n^2) = \frac{1}{2}$$

$$(e)\quad \lim_{\min\{M,N\}\to\infty} \frac{1}{MN}\sum_{m=1}^{M}\sum_{n=1}^{N}\cos(\omega_1 m+\omega_2 n)\sin(\psi_1 m+\psi_2 n) = 0$$

$$(f)\quad \lim_{\min\{M,N\}\to\infty} \frac{1}{MN}\sum_{m=1}^{M}\sum_{n=1}^{N}\cos(\omega_1 m^2+\omega_2 n^2)\sin(\psi_1 m^2+\psi_2 n^2) = 0$$

$$(g)\quad \lim_{\min\{M,N\}\to\infty} \frac{1}{MN}\sum_{m=1}^{M}\sum_{n=1}^{N}\sin(\omega_1 m^2+\omega_2 n^2)\sin(\psi_1 m^2+\psi_2 n^2) = 0$$

Proof: See Lahiri [22].

Appendix B: Proof of Asymptotic Properties

To prove the asymptotic results we need the following Lemmas.

Lemma 2: Let $\{e(m,n); m,n = 1,2,\ldots\}$ be a sequence of i.i.d. $N(0,\sigma^2)$ random variables.

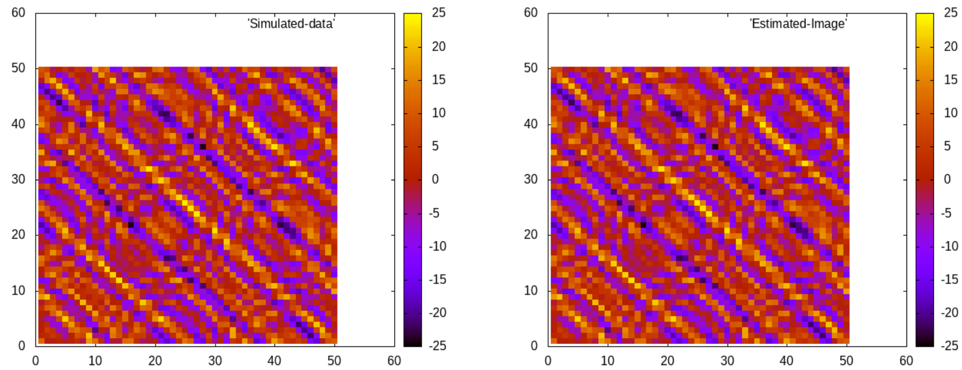

(a) (b)

Figure 7: (a) Contour plot of two-dimensional chirp-like model (7) with the model parameters (32) and (b) Contour plot of the estimated signal based on the estimated parameters.

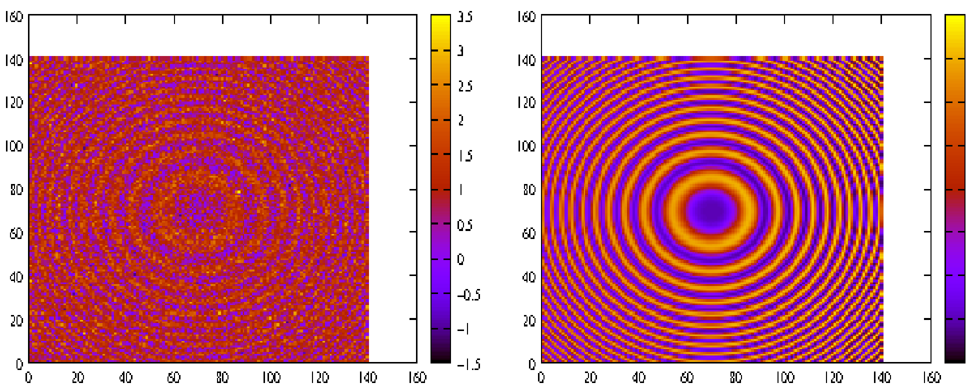

(a) (b)

Figure 8: (a) The noisy Newton Ring and (b) The estimated Newton ring.

Then as $\min\{M,N\} \longrightarrow \infty$,

$$\sup_{0<\alpha,\beta<\pi}\left|\frac{1}{MN}\sum_{m=1}^{M}\sum_{n=1}^{N} e(m,n)\cos(m\alpha+n\beta)\right| \longrightarrow 0, \quad a.s.$$

Here, '$a.s.$' denotes the almost sure convergence. The same result holds when $\cos(m\alpha+n\beta)$ is replaced by $\sin(m\alpha+n\beta)$.

Proof: The result follows from the Lemma 2 of Kundu and Nandi [20].

Lemma 3: Let $\{e(m,n); m,n=1,2,\ldots\}$ be a sequence of i.i.d. $\mathrm{N}(0,\sigma^2)$ random variables.

Then as $\min\{M,N\} \longrightarrow \infty$,

$$\sup_{0<\alpha,\beta<\pi} \left| \frac{1}{MN} \sum_{m=1}^{M} \sum_{n=1}^{N} e(m,n) \cos(m^2\alpha + n^2\beta) \right| \longrightarrow 0, \quad a.s.$$

The same result holds when $\cos(m^2\alpha + n^2\beta)$ is replaced by $\sin(m^2\alpha + n^2\beta)$.

Proof: It can be obtained from Lemma 5.2.3 of Lahiri [22].

Proof of Theorem 1: Let us consider

$$\begin{aligned}
R(\boldsymbol{\theta},\boldsymbol{\nu},\boldsymbol{\xi},\boldsymbol{\eta}) &= \frac{1}{MN} Q(\boldsymbol{\theta},\boldsymbol{\nu},\boldsymbol{\xi},\boldsymbol{\eta}) \\
&= \frac{1}{MN} \sum_{m=1}^{M} \sum_{n=1}^{N} \left(y(m,n) - f(m,n,\boldsymbol{\theta},\boldsymbol{\nu}) - g(m,n,\boldsymbol{\xi},\boldsymbol{\eta})\right)^2 \\
&= \frac{1}{MN} \sum_{m=1}^{M} \sum_{n=1}^{N} \big(f(m,n,\boldsymbol{\theta}^0,\boldsymbol{\nu}^0) - f(m,n,\boldsymbol{\theta},\boldsymbol{\nu})\big)^2 + \\
&\quad \frac{1}{MN} \sum_{m=1}^{M} \sum_{n=1}^{N} \big(g(m,n,\boldsymbol{\xi}^0,\boldsymbol{\eta}^0) - g(m,n,\boldsymbol{\xi},\boldsymbol{\eta})\big)^2 + \\
&\quad \frac{2}{MN} \sum_{m=1}^{M} \sum_{n=1}^{N} (f(m,n,\boldsymbol{\theta}^0,\boldsymbol{\nu}^0) - f(m,n,\boldsymbol{\theta},\boldsymbol{\nu})) \times ((g(m,n,\boldsymbol{\xi}^0,\boldsymbol{\eta}^0) - g(m,n,\boldsymbol{\xi},\boldsymbol{\eta})) + \\
&\quad \frac{2}{MN} \sum_{m=1}^{M} \sum_{n=1}^{N} e(m,n)(f(m,n,\boldsymbol{\theta}^0,\boldsymbol{\nu}^0) - f(m,n,\boldsymbol{\theta},\boldsymbol{\nu})) + \\
&\quad \frac{2}{MN} \sum_{m=1}^{M} \sum_{n=1}^{N} e(m,n)((g(m,n,\boldsymbol{\xi}^0,\boldsymbol{\eta}^0) - g(m,n,\boldsymbol{\xi},\boldsymbol{\eta})) + \frac{1}{MN} \sum_{m=1}^{M} \sum_{n=1}^{N} e^2(m,n).
\end{aligned}$$

Let us denote the parameter space of $(\boldsymbol{\theta},\boldsymbol{\nu},\boldsymbol{\xi},\boldsymbol{\eta})$ by $\boldsymbol{\Gamma}$, where

$$\boldsymbol{\Gamma} = [-K,K] \times [-K,K] \times [0,\pi] \times [0,\pi] \times [-K,K] \times [-K,K] \times [0,\pi] \times [0,\pi],$$

and let us consider the following set for $\epsilon > 0$;

$$\begin{aligned} S_\epsilon \;=\; & \{(\boldsymbol{\theta},\boldsymbol{\nu},\boldsymbol{\xi},\boldsymbol{\eta});(\boldsymbol{\theta},\boldsymbol{\nu},\boldsymbol{\xi},\boldsymbol{\eta}) \in \boldsymbol{\Gamma}, |A - A^0| > \epsilon\} \cup \\ & \{(\boldsymbol{\theta},\boldsymbol{\nu},\boldsymbol{\xi},\boldsymbol{\eta});(\boldsymbol{\theta},\boldsymbol{\nu},\boldsymbol{\xi},\boldsymbol{\eta}) \in \boldsymbol{\Gamma}, |B - B^0| > \epsilon\} \cup \\ & \{(\boldsymbol{\theta},\boldsymbol{\nu},\boldsymbol{\xi},\boldsymbol{\eta});(\boldsymbol{\theta},\boldsymbol{\nu},\boldsymbol{\xi},\boldsymbol{\eta}) \in \boldsymbol{\Gamma}, |\alpha - \alpha^0| > \epsilon\} \cup \\ & \{(\boldsymbol{\theta},\boldsymbol{\nu},\boldsymbol{\xi},\boldsymbol{\eta});(\boldsymbol{\theta},\boldsymbol{\nu},\boldsymbol{\xi},\boldsymbol{\eta}) \in \boldsymbol{\Gamma}, |\beta - \beta^0| > \epsilon\} \cup \\ & \{(\boldsymbol{\theta},\boldsymbol{\nu},\boldsymbol{\xi},\boldsymbol{\eta});(\boldsymbol{\theta},\boldsymbol{\nu},\boldsymbol{\xi},\boldsymbol{\eta}) \in \boldsymbol{\Gamma}, |C - C^0| > \epsilon\} \cup \\ & \{(\boldsymbol{\theta},\boldsymbol{\nu},\boldsymbol{\xi},\boldsymbol{\eta});(\boldsymbol{\theta},\boldsymbol{\nu},\boldsymbol{\xi},\boldsymbol{\eta}) \in \boldsymbol{\Gamma}, |D - D^0| > \epsilon\} \cup \\ & \{(\boldsymbol{\theta},\boldsymbol{\nu},\boldsymbol{\xi},\boldsymbol{\eta});(\boldsymbol{\theta},\boldsymbol{\nu},\boldsymbol{\xi},\boldsymbol{\eta}) \in \boldsymbol{\Gamma}, |\gamma - \gamma^0| > \epsilon\} \cup \\ & \{(\boldsymbol{\theta},\boldsymbol{\nu},\boldsymbol{\xi},\boldsymbol{\eta});(\boldsymbol{\theta},\boldsymbol{\nu},\boldsymbol{\xi},\boldsymbol{\eta}) \in \boldsymbol{\Gamma}, |\delta - \delta^0| > \epsilon\}. \end{aligned}$$

With some lengthy but straight forward calculations by using Lemma 1 repeatedly, it can be shown that for all $\epsilon > 0$

$$\liminf \inf_{(\boldsymbol{\theta},\boldsymbol{\nu},\boldsymbol{\xi},\boldsymbol{\eta}) \in S_\epsilon} R(\boldsymbol{\theta},\boldsymbol{\nu},\boldsymbol{\xi},\boldsymbol{\eta}) > \sigma^2. \tag{33}$$

For this proof only let us use the notations $\widehat{\boldsymbol{\theta}}_{MN}, \widehat{\boldsymbol{\nu}}_{MN}, \widehat{\boldsymbol{\xi}}_{MN}, \widehat{\boldsymbol{\eta}}_{MN}$ as the LSEs of $\boldsymbol{\theta}^0$, $\boldsymbol{\nu}^0$, $\boldsymbol{\xi}^0$ and $\boldsymbol{\eta}^0$, respectively. Suppose $\widehat{\boldsymbol{\theta}}_{MN}, \widehat{\boldsymbol{\nu}}_{MN}, \widehat{\boldsymbol{\xi}}_{MN}, \widehat{\boldsymbol{\eta}}_{MN}$ are not consistent estimators of $\boldsymbol{\theta}^0$, $\boldsymbol{\nu}^0$, $\boldsymbol{\xi}^0$ and $\boldsymbol{\eta}^0$, respectively. Then there exists an $\epsilon > 0$ and a subsequence of (M_k, N_k) of (M, N), such that for all $k \geq 1$,

$$(\widehat{\boldsymbol{\theta}}_{M_kN_k}, \widehat{\boldsymbol{\nu}}_{M_kN_k}, \widehat{\boldsymbol{\xi}}_{M_kN_k}, \widehat{\boldsymbol{\eta}}_{M_kN_k}) \in S_\epsilon.$$

Note that for all $k \geq 1$,

$$R(\widehat{\boldsymbol{\theta}}_{M_kN_k}, \widehat{\boldsymbol{\nu}}_{M_kN_k}, \widehat{\boldsymbol{\xi}}_{M_kN_k}, \widehat{\boldsymbol{\eta}}_{M_kN_k}) \leq R(\boldsymbol{\theta}^0, \boldsymbol{\nu}^0, \boldsymbol{\xi}^0, \boldsymbol{\eta}^0), \tag{34}$$

as $(\widehat{\boldsymbol{\theta}}_{M_kN_k}, \widehat{\boldsymbol{\nu}}_{M_kN_k}, \widehat{\boldsymbol{\xi}}_{M_kN_k}, \widehat{\boldsymbol{\eta}}_{M_kN_k})$ is the LSE of $(\boldsymbol{\theta}^0, \boldsymbol{\nu}^0, \boldsymbol{\xi}^0, \boldsymbol{\eta}^0)$ for $M = M_k$ and $N = N_k$. As $k \to \infty$, the left hand side of (34) converges to a number which is strictly greater than σ^2 due to (33), where as the right hand side converges to σ^2, which is a contradiction. Hence, $(\widehat{\boldsymbol{\theta}}_{MN}, \widehat{\boldsymbol{\nu}}_{MN}, \widehat{\boldsymbol{\xi}}_{MN}, \widehat{\boldsymbol{\eta}}_{MN})$ is a consistent estimator of ($\boldsymbol{\theta}^0$, $\boldsymbol{\nu}^0$, $\boldsymbol{\xi}^0$ and $\boldsymbol{\eta}^0$). ∎

Proof of Theorem 2: To prove Theorem 2, let us use the notation $\boldsymbol{\Theta} = (\boldsymbol{\theta}, \boldsymbol{\nu}, \boldsymbol{\xi}, \boldsymbol{\eta})$. Note that here $\boldsymbol{\Theta}$ is a 1×8 dimensional vector. Further, $\widehat{\boldsymbol{\Theta}}$ and $\boldsymbol{\Theta}^0$ have the usual meaning. Then by using multivariate Taylor series expansion of $Q'(\widehat{\boldsymbol{\Theta}})$ around $Q'(\boldsymbol{\Theta}^0)$ we obtain;

$$(Q'(\widehat{\boldsymbol{\Theta}}) - Q'(\boldsymbol{\Theta}^0)) = (\widehat{\boldsymbol{\Theta}} - \boldsymbol{\Theta}^0)Q''(\overline{\boldsymbol{\Theta}}), \tag{35}$$

here $Q'(\boldsymbol{\Theta})$ denotes the 1×8 dimensional gradient vector as

$$Q'(\boldsymbol{\Theta}) = \left[\frac{\partial Q(\boldsymbol{\Theta})}{\partial A}, \frac{\partial Q(\boldsymbol{\Theta})}{\partial B}, \frac{\partial Q(\boldsymbol{\Theta})}{\partial \alpha}, \frac{\partial Q(\boldsymbol{\Theta})}{\partial \beta}, \frac{\partial Q(\boldsymbol{\Theta})}{\partial C}, \frac{\partial Q(\boldsymbol{\Theta})}{\partial D}, \frac{\partial Q(\boldsymbol{\Theta})}{\partial \gamma}, \frac{\partial Q(\boldsymbol{\Theta})}{\partial \delta}\right],$$

$Q''(\boldsymbol{\Theta})$ denotes the 8×8 double derivative matrix defined in the standard manner and $\overline{\boldsymbol{\Theta}}$ is a point on the line joining $\widehat{\boldsymbol{\Theta}}$ and $\boldsymbol{\Theta}^0$. Now let us define the 8×8 diagonal matrix $\boldsymbol{D}$ as

$$\boldsymbol{D} = \begin{bmatrix} \boldsymbol{D}_1 & \mathbf{0} \\ \mathbf{0} & \boldsymbol{D}_2 \end{bmatrix},$$

where both $\boldsymbol{D}_1$ and $\boldsymbol{D}_2$ are 4×4 diagonal matrices as follows

$$\begin{aligned} \boldsymbol{D}_1 &= \operatorname{diag}\{M^{-1/2}N^{-1/2}, M^{-1/2}N^{-1/2}, M^{-3/2}N^{-1/2}, M^{-1/2}N^{-3/2}\} \\ \boldsymbol{D}_2 &= \operatorname{diag}\{^{-1/2}N^{-1/2}, M^{-1/2}N^{-1/2}, M^{-5/2}N^{-1/2}, M^{-1/2}N^{-3/2}\}. \end{aligned}$$

Now from (35) using that $Q'(\boldsymbol{\Theta}^0) = \mathbf{0}$, we obtain

$$[Q'(\widehat{\boldsymbol{\Theta}})\boldsymbol{D}](\boldsymbol{D}Q''(\overline{\boldsymbol{\Theta}})\boldsymbol{D})^{-1} = (\widehat{\boldsymbol{\Theta}} - \boldsymbol{\Theta}^0)\boldsymbol{D}^{-1}.$$

If we use 8×8 matrix $\boldsymbol{\Sigma}$ as

$$\boldsymbol{\Sigma} = \begin{bmatrix} \boldsymbol{\Sigma}_1 & \mathbf{0} \\ \mathbf{0} & \boldsymbol{\Sigma}_2 \end{bmatrix},$$

then using Central limit theorem and using Lemma 1 it can be shown that

$$Q'(\widehat{\boldsymbol{\Theta}})\boldsymbol{D} \xrightarrow{d} N_8(\mathbf{0}, 2\sigma^2\boldsymbol{\Sigma}). \tag{36}$$

Also, using Theorem 1 and Lemma 1 it can be shown that

$$\boldsymbol{D}Q''(\overline{\boldsymbol{\Theta}})\boldsymbol{D} \to \boldsymbol{\Sigma}. \tag{37}$$

Now combining (36) and (37), the result follows. ∎

Theorem 3: By using Lemma 1 and by similar technique as the proof of Theorem 1, it can also be established. The details are avoided. ∎

Theorem 4: By using Lemma 1 and by similar technique as the proof of Theorem 2, it can also be established. The details are avoided. ∎

Data Availability and Conflict of Interest Statement

No real data has been used in this paper. The author does not have any conflict of interest in the preparation of this manuscript.

References

[1] Abatzoglou, T. (1986), "Fast maximum likelihood joint estimation of frequency and frequency rate", *IEEE Transactions on Aerospace and Electronic Systems*, vol. 22, 708 – 714.

[2] Abratkiewicz, K. (2017), "Sonar pulse detection using chirp rate estimation and CFAR algorithms", *Hydroacoustics*, 20, 7–12.

[3] Barbarossa, S., Di Lorenzo, P. and Vecchiarelli, P. (2014), "Parameter estimation of 2D multi-component polynomial phase signals: An application to SAR imaging of moving targets", *IEEE Transactions on Signal Processing*, vol. 62, no. 17, pp. 4375–4389.

[4] Barbieri, M. M. and P. Barone (1992), "A two dimensional Prony's method for spectral estimation", *IEEE Transactions on Signal Processing*, vol. 40, 2747–2756.

[5] Binz, M., Bruder, L., Chen, L., Gelin, M.F., Domcke, W., Stienkemeier, F. (2020), “Effects of high pulse intensity and chirp in two-dimensional electronic spectroscopy of an atomic vapor” *Optics Express*, vol. 28, no. 18, Paper no. 25806.

[6] Dhar, S.S., Kundu, D. and Das, U. (2019), “On testing parameters of chirp signal model”, *IEEE Transactions on Signal Processing*, vol. 67, no. 16, 4291 – 4301.

[7] Djuric, P.M. and Kay, S.M. (1990), “Parameter estimation of chirp signals”, *IEEE Trans. on Acoustics, Speech and Signal Processing*, vol. 38, no. 12, 2118–2126.

[8] Francos, J. M., Meiri, A. Z., and Porat, B. (1993), “A unified texture model based on a 2-D Wald-like decomposition, *IEEE Transactions on Signal Processing*, vol. 41, no. 8, 2665–2678.

[9] Gini, F., Montanari, M. and Verrazzani, L. (2000), “Estimation of chirp signals in compound Gaussian clutter: A cyclostationary approach”, *IEEE Transactions on Acoustics, Speech and Signal Processing*, vol. 48, 1029 – 1039.

[10] Grover, R. (2019), “Frequency and frequency rate estimation of some non-stationary signal processing models”, *Ph.D. thesis at Indian Institute of Technology, Kanpur*, India. https://etd.iitk.ac.in:8443/jspui/handle/123456789/18684.

[11] Grover, R., Kundu, D. and Mitra, A. (2018), “On approximate least squares estimators of parameters on one dimensional chirp signal”, *Statistics*, vol. 52, no. 5, 1060 – 1085.

[12] Grover, R., Kundu, D. and Mitra, A. (2018), “Asymtotic of approximate least squares estimators of parameters of two-dimensional chirp signal”, *Journal of Multivariate Analysis*, vol. 168, 211 - 220.

[13] Grover, R., Kundu, D. and Mitra, A. (2021), "An efficient methodology to estimate the parameters of a two-dimensional chirp signal model", *Multidimensional Systems and Signal Processing*, vol. 32, no. 1, 49 - 75.

[14] Grover, R., Kundu, D. and Mitra, A. (2021), "Asymptotic properties of least squares estimators and sequential least squares estimators of a chirp-like signal model parameters", *Circuits, Systems and Signal Processing*, vol. 40, no. 11, 5421 – 5467.

[15] Guo, Y. and Yang, L-D. (2020), "Chirp-Fourier transform for quadratic phase interference fringe analysis: Principles, method and application", *Optics and Lasers in Engineering*, ol. 133, Paper No. 106145.

[16] Guo, Z., Lu, M-F., Wu, J-M., Jin, X-W., Zhang, F. and Tao, R. (2019), "Fast FRFT-based method for estimating physical parameters from Newton's rings", *Applied Optics*, vol. 58, No. 14, 3926 – 3931.

[17] Hua, Y. (1992), "Estimating two dimensional frequencies by matrix enhancement and matrix pencil", *IEEE Transaction on Signal Processing*, vol. 40, 2267-2280.

[18] Jia, Z., Zheng, W. and Yuan, F. (2022), "A Two-Dimensional Chirp-MFCSK Modulation Method for Underwater LoRa System, *IEEE Internet of Things Journal*, vol. 9, NO. 23, 1.

[19] Kundu, D., Grover, R. and Nandi, S. (2021), "A review of chirp and some other related signal processing models", *Advances in Signal Processing: Reviews*, Vol. 2, Editor: Sergey Y. Yurish, IFSA Publishing, S.L. Barcelona, Spain, pp 149 - 233. ISBN: 978-84-09-28830-4, 2021.

[20] Kundu, D. and Nandi, S. (2003), "Determination of Discrete Spectrum in a Stationary Random Field", *Statistica Neerlandica*, vol. 57, no. 2, 258–284.

[21] Kundu, D. and Nandi, S. (2008), "Parameter estimation of chirp signals in presence of stationary noise", *Statistica Sinica*, vol. 18, no. 1, 187 - 201.

[22] Lahiri, A. (2011) *Estimators of Parameters of Chirp Signals and Their Properties*, Ph.D. Thesis, Indian Institute of Technology Kanpur, India, https://etd.iitk.ac.in:8443/jspui/handle/123456789/12724.

[23] Lahiri, A., Kundu, D and Mitra, A. (2012), "Efficient algorithm for estimating the parameters of chirp signal", *Journal of Multivariate Analysis*, vol. 108, 15–27.

[24] Lahiri, A., Kundu, D. and Mitra, A. (2014), "On least absolute deviation estimator of one dimensional chirp model", *Statistics*, vol. 48, no. 2, 405 – 420.

[25] Lahiri, A., Kundu, D. and Mitra, A. (2015), "Estimating the parameters of multiple chirp signals", *Journal of Multivariate Analysis*, vol. 139, 189 – 205.

[26] Mittal, A., Kundu, D., Mitra, A. and Grover, R. (2023), "Estimation of the Elementary Chirp Model Parameters", *IEEE Transactions on Aerospace and Electronic Systems*, vol. 59, no. 5, 5218 – 5234.

[27] Mittal, A., Grover, R., Kundu, D. and Mitra, A. (2023), "Efficient methodology for estimating elementary chirp model parameters", *IEEE Transactions on Signal Processing*, vol. 71, 2352 – 2365.

[28] Mittal, A., Grover, R., Kundu, D. and Mitra, A. (2023), "Estimation of the Elementary Chirp Model Parameters", *IEEE Transactions on Aerospace and Electronic Systems*, 2023.

[29] Nandi, S., Grover, R. and Kundu, D. (2021), "Estimation of Parameters of Multiple Chirp Signal in Presence of Additive Alpha-Stable Errors", *Signal Processing*, vol.189, Paper no. 108232.

[30] Nandi, S. and Kundu, D. (2004), "Asymptotic properties of the least squares estimators of the parameters of the Chirp signals", *Annals of the Institute of Statistical Mathematics*, vol. 56, no. 3, 529–544.

[31] Nandi, S. and Kundu, D. (2020), "Estimation of parameters in random amplitude chirp signal", *Signal Processing*, vol. 168, Art. 107328.

[32] Nandi, S. and Kundu, D. (2020), *Statistical Signal Processing: Frequency Estimation*, Springer, Singapore.

[33] Quinn, B.G. and Hannan, E.J. (2001),*The Estimation and Tracking of Frequency*, Cambridge University Press, Cambridge, United Kingdom.

[34] Rao C. R., L. C. Zhao and B. Zhou (1994), "Maximum likelihood estimation of 2-D super- imposed exponential signals", *IEEE Transaction on Acoustics, Speech and Signal Processing*, 42, 1795–1802.

[35] Rihaczek, A.W. (1969), *Principles of High Resolution Radar*, New York McGraw Hill, USA.

[36] Saha, S. and Kay, S. (2002), "Maximum likelihood parameter estimation of superimposed chirps using Monte Carlo importance sampling", *IEEE Transactions on Signal Processing*, vol. 50, 224 – 230.

[37] Shukla, A., Grover, R., Kundu, D. and Mitra, A. (2023), "A computationally efficient algorithm to estimate the parameters of a two-dimensional chirp model", *Multidimensional Sysytems and Signal Processing*, vol. 34, 633 – 655.

[38] Tekavec, P.F., Myers, J.A., Lewis, K.L.M., Fuller, F.D. and Ogilvie, J.P. (2010),"Effects of chirp on two-dimensional Fourier transform electronic spectra", *Optics Express*, vol. 18, No. 11, Paper no. 11015.

[39] Vangelista, L. (2017), "Frequency shift chirp modulation: The LoRa modulation", *IEEE Transactions on Signal Processing Letters*, vol. 24, no. 12, 1818–1821.